2014 IEEE International Conference on Robotics & Automation (ICRA)
Hong Kong Convention and Exhibition Center
May 31 - June 7, 2014. Hong Kong, China

Multi-joint Actuation Platform for Lower Extremity Soft Exosuits

Ye Ding, Ignacio Galiana, Alan Asbeck, Brendan Quinlivan, Stefano Marco Maria De Rossi, Conor Walsh, *Member, IEEE*

***Abstract*—Lower-limb wearable robots have been proposed as a means to augment or assist the wearer's natural performance, in particular, in the military and medical field. Previous research studies on human-robot interaction and biomechanics have largely been performed with rigid exoskeletons that add significant inertia to the lower extremities and provide constraints to the wearer's natural kinematics in both actuated and non-actuated degrees of freedom. Actuated lightweight soft exosuits minimize these effects and provide a unique opportunity to study human-robot interaction in wearable systems without affecting the subjects underlying natural dynamics. In this paper, we present the design and control of a reconfigurable multi-joint actuation platform that can provide biologically realistic torques to ankle, knee, and hip joints through lower extremity soft exosuits. Two different soft exosuits have been designed to deliver assistive forces through Bowden cable transmission to the ankle and hip joints. Through human subject experiments, it is demonstrated that with a real-time admittance controller, accurate force profile tracking can be achieved during walking. The average energy delivered to the test subject was calculated while walking at 1.25 m/s and actuated with 15% of the total torque required by the biological joints. The results show that the ankle joint received an average of 3.02J during plantar flexion and that the hip joint received 1.67J during flexion each gait cycle. The efficiency of the described suit and controller in transferring energy to the human biological joints is 70% for the ankle and 48% for the hip.**

I. Introduction

Research in powered exoskeleton devices with the goal of assisting or enhancing human activities, began in the late 1960s [1]. Over the last two decades, a number of lower extremity robotic exoskeletons have been proposed for military-targeted power and endurance augmentation [2-4], rehabilitation [5-13] and functional replacement [14].

These previous exoskeletons typically rely on rigid linkages parallel to the biological anatomy. Pads, straps, belts, vacuumed sockets or other techniques are used to couple the body with the exoskeletons. Due to the rigid linkages, large inertia and corresponding joints misalignments, the traditional rigid exoskeletons constrain the biological joints of the actuated and non-actuated degrees of freedom (DOFs), which leads to deviation from the wearer's natural motion, discomfort or injuries [15, 16]. Moreover, an additional consequence is that a wearer will typically expend an increased amount of energy to complete a desired motion (e.g. walking). Although various controllers have been designed to provide a more intimate and natural interaction between the device and the wearer, these effects still limit the applicability of these systems outside of a laboratory environment.

To address these limitations, there has been a recent push to develop next generation wearable robots that use soft materials such as textiles and elastomers to provide a more conformal, unobtrusive and compliant means to interface to the human body [17, 18]. Unlike traditional exoskeletons which contain rigid linkage elements, the vision is that these systems can be worn like clothing; yet still generate significant moments at the leg joints to assist with walking. Compared to traditional exoskeletons, the wearer's joints are unconstrained by external rigid structures, and the worn part of the suit is extremely light, which minimizes the suit's unintentional interference with the body's natural biomechanics.

Early work in soft wearable robots utilized McKibben actuators to attach to the soft suit and generate forces across the biological joints [17, 19]. The reasons for selecting McKibben actuators for these systems are that they are compliant, yet can still generate significant forces to mimic those from the underlying biological muscles and for early prototyping, the power source can be off the wearer and connected via a tether. However, a limitation of McKibben actuators is that their stroke length is limited, meaning that the soft exosuit can pose constraints on the human body. This can be a particular challenge when antagonistic actuation is

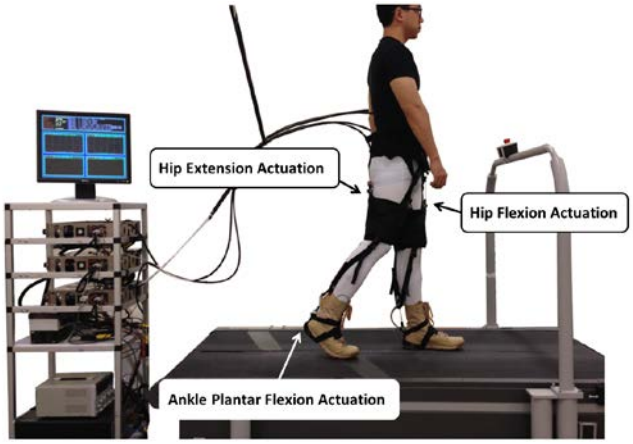

Figure 1 Multi-joint actuation platform with ankle and hip soft exosuit

*This material is based upon work supported by the Defense Advanced Research Projects Agency (DARPA), Warrior Web Program (Contract No. W911QX-12-C-0084). The views and conclusions contained in this document are those of the authors and should not be interpreted as representing the official policies, either expressly or implied, of DARPA or the U.S.Government. This work was also partially funded by the Wyss Institute for Biologically Inspired Engineering and the School of Engineering and Applied Sciences at Harvard University.

Y. Ding, I. Galiana, A. Asbeck, S.M.M. De Rossi, C. Walsh are with the School of Engineering and Applied Science, Harvard University, Cambridge, MA 02138 USA (phone: 617-496-7128, email: walsh@seas.harvard.edu)

B. Quinlivan is with Franklin W. Olin College of Engineering, Needham, MA, 02492

Corresponding author: C. J. Walsh

required. In addition to affecting the range of motion, accurate position and force control is hard to achieve for this form of actuation.

To alleviate some of these challenges, a system with a cable-based actuation system was introduced. Bowden cables are used to transmit forces from proximally mounted electromechanical actuation units to distal attachment points on the soft suit to assist the lower extremities. A torque can be applied to the biological joint by attaching the end of the Bowden cable sheath and inner cable on either side of it. When the Bowden cable is actuated, it brings together these attachment points, thus generating a pulling force on the suit and a resultant torque at the joint. Since Bowden cables can be configured to follow any path, this allows flexibility in the placement of the actuator units. For example, they could be mounted on a waist belt, backpack or even on a lab bench.

The combination of a soft textile exosuit and low profile remote actuation means that for the first time torques can be applied to the lower extremities without adversely affecting the natural dynamics and degrees of freedom of walking. While, there has been much exciting prototype development in the area of wearable robotics, many basic scientific research questions remain to understand the required characteristics of the assistive torques to be applied the user in order to improve locomotor performance. These systems need to be highly intuitive to the wearer, provide assistance when required while providing minimal to no disruption the rest of the time so as to not interfere with the human natural gait and biomechanics. In particular, they should sync synergistically with the user so that natural movement and stable control can be achieved while inputting minimal actuator energy.

To explore these human-robot interaction research questions in an efficient and controlled manner, we present a laboratory-based reconfigurable off-board multi-joint actuation platform that can be connected to lower extremity soft exosuits as shown in Figure 1. With this platform, the weight of the actuation system does not affect our exploration of the optimal means to apply assistance. The control strategies developed on this platform will be used in our future fully-mobile systems. This platform consists of six linear actuators connected to Bowden cables which are designed to provide biologically realistic torques either separately or simultaneously at the ankle, knee and hip joints during normal walking. Since our goal is to provide torques in parallel to muscle groups as opposed to controlling the position of the joint, our systems don't necessary require two actuators for each joint. In this paper, two different exosuits are presented actuating ankle plantar flexion and hip flexion/extension respectively. Using a real-time control architecture, it is demonstrated that accurate assistive forces can be delivered to the human joints through soft exosuits with an admittance controller. The actuation platform has integrated sensors that monitor voltage, current, force and position at the actuator-side and a force sensor in the exosuit to monitor local forces so that electrical and mechanical energy calculations can be performed. This allows the calculation of the actuation efficiency, the amount of power delivered by the actuators to the suit and the efficiency of the suit in transmitting power to the biological joints. Experimental walking test results on human subjects show that the proposed system can deliver accurate forces to multiple joints through soft exosuits.

II. Soft Exosuit for Gait Assistance

The soft exosuits discussed in this paper were designed to provide appropriate assistance to the lower extremity joints through a comfortable user interface, improving the wearer's walking efficiency and reducing the muscular effort. We focus on actuating the ankle and hip independently but in the future we envision a system that assists multiple joints simultaneously during walking. Although the determinants of efficient assistance are largely unknown, the strategy of adding external torques to supplement normal muscle work to the lower limb joints has been applied with success in previous research [17, 20, 21]. The designed multi-joint actuation platform can be used to provide torques to the lower limb via soft exosuits and explore different assistive strategies and their implications to human biomechanics.

A. Design Principles for Soft Exosuits

In general, an exosuit should be able to create paths to transfer load between the assisted joint and other parts of the body where those forces can be handled without impeding natural human walking dynamics and comfort. In previous work we have described design principles that can be used to achieve this and demonstrated it with functional prototypes [18, 22]. Reaction forces created during the actuation should be distributed along the suit to minimize the normal pressure. In addition, the suit should not restrict muscles from expanding during operation. High suit stiffness is required to optimize power transfer efficiency and reduce the risk of

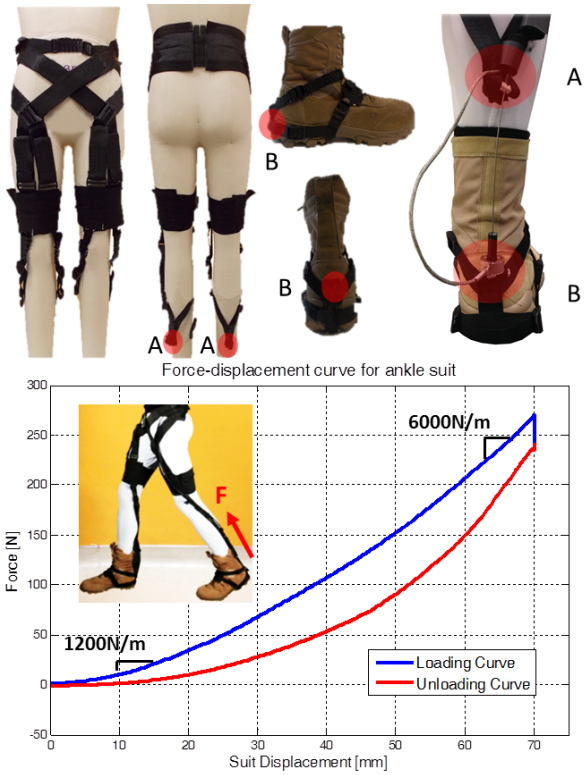

Figure 2 Ankle exosuit for plantar flexion actuation and exosuit stiffness

chafing. The peak force that can be generated during each gait cycle is also partially dependent on the suit stiffness. Since the activation time of the ankle flexor is very short for each gait cycle, it requires the actuator to stretch the compliant exosuits quickly enough to achieve the desired assistive force, which means the softer the exosuit, the higher the speed needed by the actuator.

B. Ankle Suit (Plantar flexion)

A suit dedicated to actuating the ankle joint has been designed as shown in Figure 2 as an improved version of that previously reported in [18]. The suit creates a path that allows the transfer of forces between the pelvis and the heel. It is composed of a waist belt, two thigh braces, connecting webbing straps, two boot attachments and two Bowden cable anchor points (A on top of the heel and B at the back of the boot) for each leg as shown in Figure 2.

The ankle suit waist belt is located at the pelvis area (iliac crest). It is a bony area less prone to bone-skin movements, and hence relatively large forces can be better handled compared to other parts of the body. Two webbing straps start at the waist belt and merge at a cross point at the front of the thigh. From the cross point, another two webbing straps go down to the back side of the leg passing through the thigh brace and the center of rotation of the knee. These two webbing straps merge again on at the back of the calf, forming the attachment point for the Bowden cable sheath (A), shown in Figure 2. The webbing straps around the boots and merge at the back of the heel forming the attachment point for the inner cable (B) also shown in Figure 2. When the cable is actuated, it generates a force between anchor points A and B that produces an upward tension force 6-9cm behind the ankle center of rotation, thus creating plantar flexion torque on the ankle joint. The suit also creates a flexion torque on the hip due to the tension forces in the suit passing 7-10cm in front of the hip axis of rotation. The total weight of the ankle exosuit is 915g (not including the weight of the boots).

The stiffness of the suit is defined by the properties of the fabric, the human body and the interface between the human and the suit. A stiff polyester webbing strap was selected as the main force transmission fabric of the suit. Due to the relatively high stiffness of the suit, the force can be accurately delivered to the subject and skin chafing has not been reported during the tests. A stiffness measurement for the ankle suit was performed by positioning a human subject in walking push off pose as shown in Figure 2. The average force at the ankle and displacement of the actuator over 10 cycles were recorded. As it can be seen from the plot of cable displacement versus applied force, a force of 270N force can be applied with a cable actuation of 70mm amplitude. In addition, the plot shows that the suit increases its effective stiffness up to a value of approximately 6000N/m, during the loading process.

C. Hip Suit (Flexion & Extension)

A hip exosuit that assists hip flexion and extension during walking was also designed and is shown in Figure 3. This exosuit is composed of a waist belt, two thigh braces and two stretchable webbing straps on each side of the legs for holding the thigh braces in place. One pair of anchor points (C,D) for

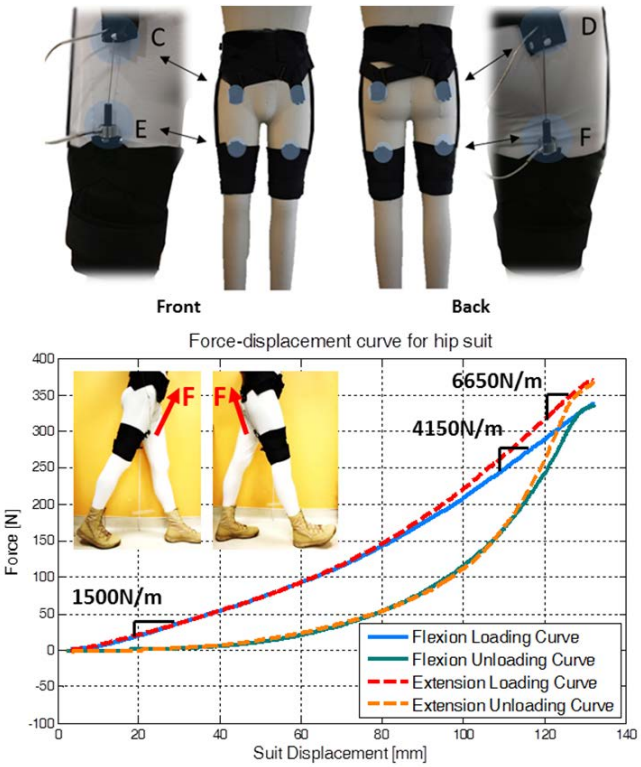

Figure 3 Hip exosuit for flexion/extension and exosuit stiffness

Bowden cable sheath attachment on both sides of the waist belt above the hip joint, and the other pair of anchor points (E, F) for inner cable attachment located at the top center on both sides of the thigh brace. Thus, the hip suit creates paths that can transfer assistive forces from the attachments on the thigh brace to the pelvis area. When the front cable is actuated, the cable applies an upward force on the front side of the hip to create a flexion torque. When the rear side cable is actuated, the cable creates an extension torque. The total weight of the hip suit is 672g.

Following the same procedure as with the ankle exosuit, the effective stiffness was measured both for flexion and for extension assistance as shown in Figure 3. The average stiffness of the hip suit is lower than the ankle suit because of the compliance of the thigh and hip muscles and the lack of a solid anatomical feature onto which the distal side of the suit can be attached (for comparison, the ankle suit connects to the boot, which is relatively rigid). For 130mm cable displacement, forces for hip flexion and extension can reach approximately 350N with effective stiffnesses of 4150N/m and 6650N/m respectively.

III. Multi-joint Actuation Platform

Given an understanding of the properties of the exosuits and normal biomechanics of human walking, a multi-joint actuation platform was designed to deliver forces to the lower-limb joints through the soft exosuits. A general picture of the system is shown in Figure 1. The platform contains three sets of identical actuation units, each with two actuated linear degrees of freedom that connect to Bowden cable attachments. The motor controllers, data acquisition card, power supply and a target PC were also installed for

TABLE I ACTUATOR BOX DESIGN SPECIFICATIONS

	Ankle	Knee	Hip
Range of motion of biolgocial joints (Deg)	27	70	29
Peak speed of biological joints (rad/s)	4.5	7.3	3.5
Biological joint moments (Nm)	130	40	104
Estimated exosuit moment arm (m)	0.085	0.07	0.1
Actuator minimum travel (m)	0.13	0.11	0.11
Actuator minimum speed (m/s)	1.5	2	1.6
Actuator peak force (N)	1466	571	1040

measuring the sensor signals and controlling the actuators. This section describes and evaluates the biological requirements for the system, the actuation platform and the different sensors integrated in the system.

A. Biological Requirements

A requirement for the actuation platform was that it should be capable of fully replicating the torques and powers at the hip, knee and ankle joint during walking. The requirements for defining torque and speed for the actuator were obtained from human gait data [23] and the effective stiffness of the suit for each joint as described in the previous section. For an 80kg subject walking at 1.25m/s, the average peak joint torque for ankle, knee and hip are 130N/m, 40N/m, and 104N/m, respectively. The average peak angular speed for those joints are 4.5rad/s, 7.3rad/s, and 3.5rad/s , calculated from the human gait data [23]. To translate torque and rotational motion into force and linear movement, the moment arm for each joint was estimated based on our current suit which was designed for 160cm-200cm height subjects with a body mass index from 20 to 30. Due to the soft textile nature of the exosuits, they can be easily adapted to anatomical variations. The minimum required speed for the actuators is the result of evaluating the effect of biological joint speed plus the extra displacement required to stretch the exosuit in order to generate the necessary forces. The biological data and resulting actuator specifications that follow the biological requirements are listed in Table 1.

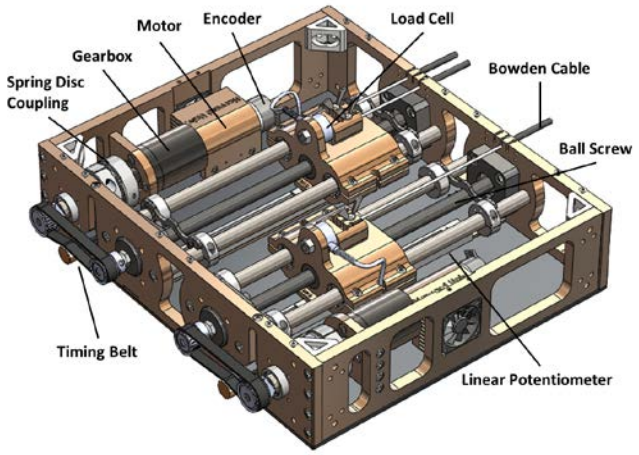

Figure 4 Modular designed reconfigurable Bowden cable actuation box

B. Mechanical Design of Bowden Cable Actuator

Based on the requirements depicted in Table 1, a Bowden cable actuator box has been designed as shown in Figure 4. The Bowden cable sheath connects to the outer frame of the actuator box and the inner cable is attached to a ball screw actuated carriage which can drive the inner cable back and forth. Three actuation boxes with different gear ratios were designed to actuate the ankle, knee and hip, or a combination of them at the same time. A Maxon EC-4 pole brushless motor and gearbox with a 4.3:1 gear ratio is attached to the aluminum frame. A spring disc coupler connects the motor shaft to another steel shaft resting on a stronger ball bearing to avoid high lateral forces on the timing belt that would damage the bearings in the gearbox. A 12.7mm pitch ball screw is connected on the other side of the timing belt pulley to translate the rotational motion into a linear movement. An aluminum carriage is thread jointed to the nut of the ball screw. It is guided by four linear ball bearings, two on each side. The Bowden cable inner wire rope is fixed to the small aluminum block and secured by a wind screw. With the Bowden cable sheath attached on the outer box frame, the linear carriage transmits its linear movement to actuate different biological joints with the exosuit.

To uphold design flexibility and enable the adaptation of the system's force/speed ratio to different joints and to different exosuit designs, the gear ratio of the actuator is easily adaptable by swapping the timing belt pulleys exposed at the rear side of the actuation box.

C. Sensing and Instrumentation

In addition to providing actuation, the system also includes sensors to enable real-time feedback control and data logging at a frequency of 1 kHz. A Maxon 4 line encoder (500 counts/rev) is installed on the back of the motor for measuring the motor speed and a linear potentiometer (P3 America, Inc.) with a resolution of 0.1mm is placed under the ball screw and connected to the carriage to measure the displacement of the actuation cable. A Futek load cell with a measuring range of ±2224N (2N resolution) is placed between the carriage and the aluminum Bowden cable block to measure the tension force in the actuation cable before the Bowden cable transmission. At the distal ends of the Bowden cable, there is another Futek load cell with a measuring range of ±1112N (1N resolution) to measure the actual force applied to the exosuit and wearer. Foot switches are placed in the boots for detecting heel strike events to characterize the phase of the gait cycle.

Matlab xPC Target was programmed by using Matlab Simulink environment for the real time control implementation. The data acquisition card PCI-6259 was selected to acquire the sensor signals and send reference voltage to the Copley ACP-090-36 Accelnet controller. Current and voltage sensors are built in the Copley Accelnet motor controller.

These sensors allow measuring the amount of energy consumed by the system, the efficiency of the mechanical transmission, and the power delivered to the human body and

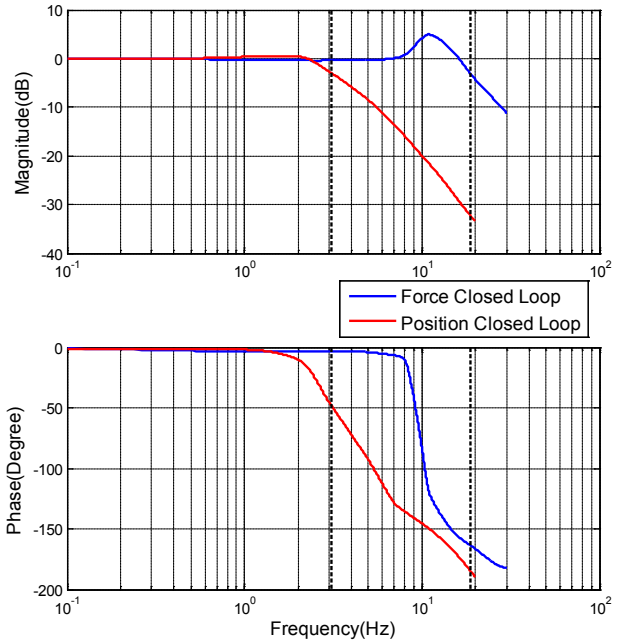

Figure 5 Actuator's bandwidth test results

to the exosuit. Therefore, the performance of the system and assistive control strategies can be evaluated with this platform.

C. Actuator Characterization

1) Actuator Bandwidth

The bandwidth of the most highly geared actuator (for the ankle joint) was evaluated experimentally to characterize the performance of the system. The actuator position and force bandwidth were measured by commanding swept sinusoidal position and force signals (from 0.1 to 30Hz) of 50mm and 100N (100mm and 200N peak to peak) for the closed-loop position and force controller. The control loops were closed using the position signals acquired from the linear potentiometer and the force signal from the load cell at the wearer-side of the Bowden cable. Both signals were filtered by a 1st order low pass filter with a cutoff frequency of 50Hz. The distal end of the Bowden cable was hanging free when implementing the position bandwidth test. However, for the force bandwidth test, the distal end of the inner cable with the load cell and the cable sheath were fixed to a rigid element. Magnitudes and phases of the reference signal and output signals were recorded at each frequency. The closed loop system magnitude and phase were obtained by comparing the recorded signals. More data points of the closed loop system were interpreted in Matlab to create a smoother presentation of the Bode plot.

The results shown in Figure 5 demonstrate that the actuator position control bandwidth is around 3Hz with a phase margin of -46˚ while the force control bandwidth is on the order of 20Hz with a phase margin of -161˚.

2) Safety

Mechanical and software protections were implemented to ensure safe operation of the system. The mechanical stops on the actuator can adjust the hard limits of the actuator position over a range from 0mm to 160mm. These stops can hold up to 1500N force when fully fastened onto the stainless steel rods. In addition, there are adjustable software limits in the control box. Once the actuator reaches the safety limits, the control program will immediately send the actuator to the distal end to make the cable slack in order to avoid providing any force to the user. When delivering the assistance, the assistive force increases gradually to allow the user to get used to the system. The target force profile reaches its maximum after 3 minutes of normal walking. Due to the soft nature of the system, the compliance and elasticity protects the actuator from the shock and more importantly the assistive forces are inherently limited mechanically [24, 25]. Unsafe conditions arise when some of the sensors stop providing signals (either by loosened or worn-out wires). To address this potentially unsafe condition, a script was implemented in Matlab for comparing input signals. The DAQ reads the raw signals from the sensors, and if the program discovers a faulty or anomalous signal, the program will send the actuator to the distal end. An emergency switch which depowers all the actuators when pressed was also installed in the system. A temperature sensor was installed on each of the Maxon motor's heat sink to protect them from overheating. The system shuts down the motor controller when a motor reaches 120˚ C.

IV. Joint-Level Control

A. Force Trajectory Design and Implementation

While the actuation platform is capable of delivering 100% of the torque required to match that of the biological joints for an 80kg subject, the current exosuit designs allow 15% of the total torque required by the joint to be delivered. Figure 6 shows the required torque for the ankle and hip joints during walking for a gait cycle starting with heel strike of one leg to the next heel strike of the same leg. The force profiles are the standardized joint torques profiles adopted from [23] divided by the moment arms of the current ankle and hip exosuits. For an 80kg wearer, the 15% force trajectories would have peak forces of 240N, 130N, and 160N for ankle, hip flexion and extension respectively. The hip suit spans just the hip joint and so does not exert reacting torques to any other joint when actuated, thus the commanded force profile for the hip is the total joint force scaled by 15% as shown at the top part of Figure 6. The force profile for hip flexion is actuated from 35% to 75% of the gait cycle. The force profile commanded for hip extension actuation is the remaining portion of the hip force profile.

The force profile for actuating the ankle cannot simply be directly scaled by 15% due to the structure of the ankle suit that creates a force path between the ankle and the pelvis passing through the center of rotation of the knee and the anterior part of the hip joint. Since the suit goes through the center of rotation of the knee, no torque is provided to this joint; however, there is a corresponding hip flexion torque added while actuating the ankle joint. In order to avoid hindering the hip joint the commanded force profile to the ankle begins when the applied force benefits both joints (around 35% of the gait cycle) as shown at the bottom part of Figure 6. The reference force follows the hip flexion profile until the scaled ankle force profile intersects with the hip force profile. Thus, the force trajectory for ankle plantar flexion is a combined curve, which assists the ankle joint and hip joint

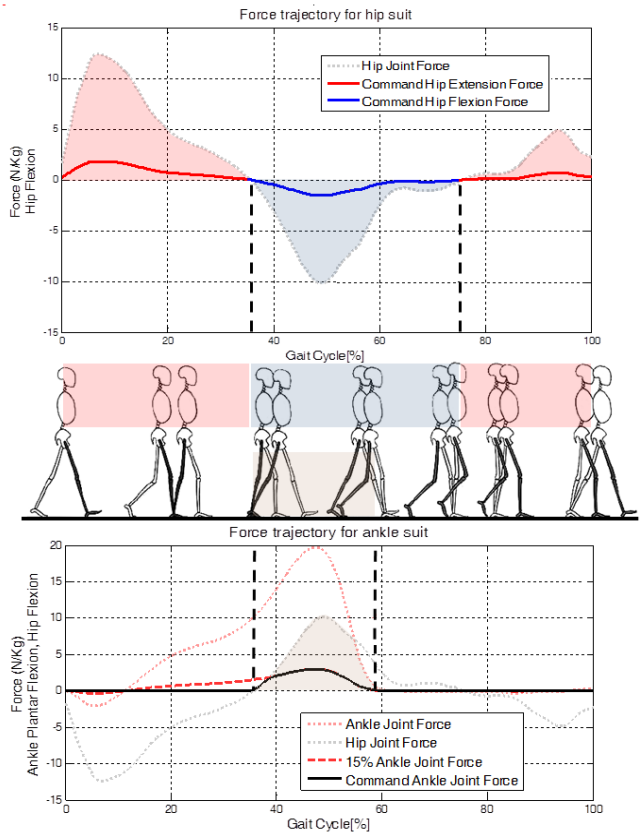

Figure 6 Force trajectory for ankle and hip soft exosuits

from 35% to 60% of the gait cycle. With this design, it is guaranteed that beneficial forces are provided simultaneously to the ankle and to the hip flexion by using only one actuator and hence increasing the system efficiency [18].

In order to implement the actuation scheme, the normalized reference force trajectories for each joint were pre-computed and saved in the controller. The control algorithm adapts those profiles by scaling them based on the step frequency obtained by the foot switches in real-time. The heel strike signal from the foot switch was used to segment the gait cycle percentage and to trigger the force control. Since there is a mechanical delay for the foot switches, the heel strike signal corresponded to 20ms after the starting point of the gait cycle.

B. Admittance Controller Design

The force control of the soft exosuits is implemented by using a position-based admittance controller with force as an input. In general, an admittance controller structure for this application is comprised of a cascade-like controller in which there is a position loop, and an outer force loop. The position and force signals are obtained from the linear potentiometer in the actuation unit and load cell on the wearer side of the Bowden cable. This allows for measurement of human-suit interaction forces to determine different virtual inertia, damping and stiffness properties for the transmitted force profile which guarantees safety and stability in the system. A distal end-point admittance controller for the Bowden cable actuator was implemented as shown in Figure 7. The virtual admittance transforms a force error into a desired position that is then sent to the inner-position control loop. The admittance equation is defined in the Laplace domain as follows:

$$Y = \frac{x}{F} = \frac{1}{M_v \cdot s^2 + b_v \cdot s + K_v}$$

Where M_v, b_v, K_v, x, F, and Y define the virtual inertia, damping, stiffness, cable displacement, local assistive force and the virtual admittance respectively. Considering that the position controller compensates for the actuator dynamics and friction, only the defined virtual mass, damping and stiffness are felt by the human [26].

In contrast to pure force control which rejects position disturbance in order to track a given reference force trajectory, the position compensator attempts to comply with the environmental interaction and react quickly to position changes of the end point by rapidly modifying the inner loop trajectory. By setting saturations on the position reference, the actuator will stop moving further if it reaches the hardware limits. The designer can define position and force limits in the system, thus reducing the potential risks of inadvertent forces to the actuator and the subject.

V. Human Walking Experiments

A pilot study, approved by the Harvard Medical School Committee on Human Studies, to study ankle plantar flexion and hip flexion assistance during treadmill walking was performed. The human subject experiments were carried out on an 80kg male subject. The admittance control described in the previous section was validated during these tests. Two trials were performed, consisting of the subject walking for 2

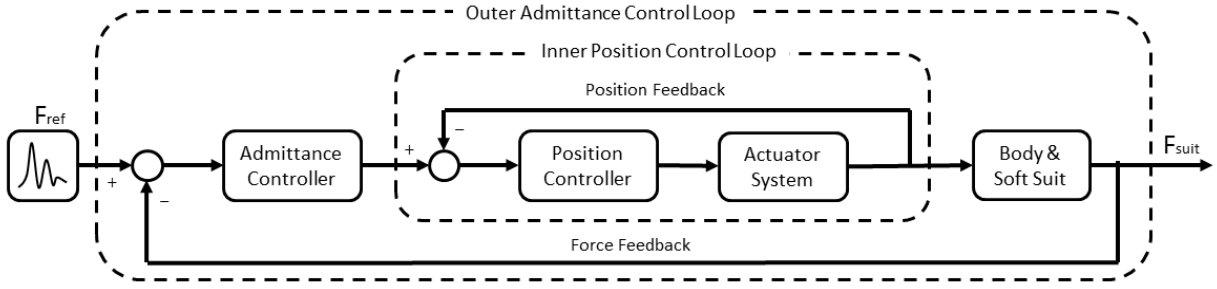

Figure 7 Block diagram of the admittance controller

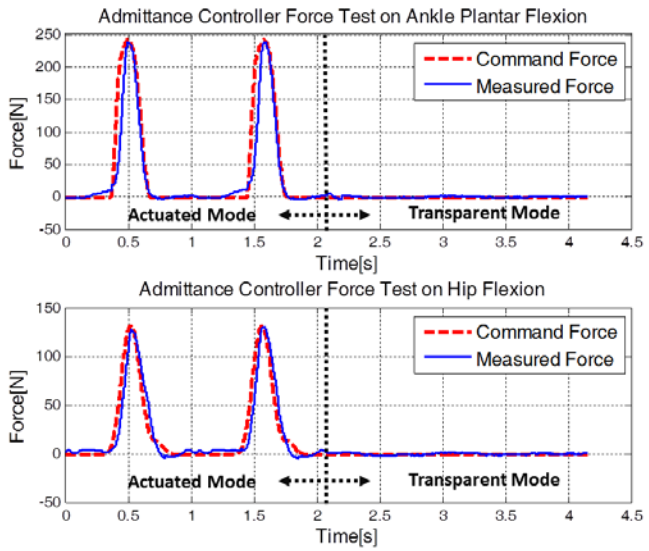

Figure 8 Admittance controller force test on the ankle plantar flexion and hip flexion

minutes while wearing the ankle and the hip flexion exosuits described in Section II. During the experiments, two conditions were considered: an assistive mode in which the actuation platform provides forces to the user during walking and a "slack" or transparent mode that consists on pushing the cable out, which allows the system to passively avoid providing any interaction forces to the user while walking. Under transparent mode, the exosuit does not constrain or apply forces to the wearer, thus it does not change the wearer's natural kinetics. Having the ability to make the suit transparent is a significant benefit of this approach as well as enabling the implementation of other strategies such as making the system transparent when a low-battery condition is detected. This approach is not possible to implement with traditional rigid exoskeletons since the user will need to take off the system in order to be able to walk freely again in the event of low-battery or power loss.

Figure 8 shows force measurements during 4 walking gait cycles consisting of 2 actuated followed by 2-non actuated (transparent mode) cycles for both exosuits (ankle plantar flexion and hip flexion). As it can be seen, the system can deliver accurate force trajectories to the wearer. In addition, when the system is commanded to be in transparent mode the measured force is 0N and hence does not impede the wearer's gait.

The corresponding total mechanical energy transmitted to the exosuit and human by the actuation platform is measured by using the total cable displacement and the local force measured at the wearer side. In order to understand the energy transfer process, it is important to know the energy flow on the exosuit. Based on the exosuit stiffness discussed in section II, the average displacement of the exosuit during a gait cycle can be calculated from the average local force profile during loading and unloading conditions; the power delivered to the exosuit can then be obtained by multiplying the measured local force and the estimated anchor point speed (derivative of the exosuit displacement). Thus, the power delivered to the joint is the total mechanical power delivered minus the power delivered to the exosuit. The power transfer process is directly related to the efficiency and performance of our system and will allow optimizing assistive strategies for future fully mobile systems.

Figure 9 shows the average power results for a gait cycle for both ankle plantar flexion and hip flexion actuation during walking. It can be seen that since the start of the actuation (35%), most of the total power delivered by the actuation platform is stored by the ankle and hip soft-exosuits until approximately 46% and 50% of the gait cycle respectively; this occurs due to the inherent compliance of the exosuit. At this point, the exosuit transfers most of the stored energy to the human biological joints. All of the energy stored is not returned due to the exosuit hysteresis as described in Section II.

For the human walking trials presented in Figure 9, the system delivered 4.01W on average over a gait cycle of 1.08 seconds with the ankle suit, and 3.27 W on average over a gait cycle of 1.06 seconds for the hip suit. The total energy delivered by the system over a single gait cycle was 4.33J and 3.47J respectively. During each gait cycle, the ankle joint received 3.02 J for an efficiency of 70%. The hip joint received 1.67 J for the flexion with an efficiency of 48%. Compared to biological joint power, the system provided 14.3% of energy needed by the ankle and 9.6% of energy needed by the hip for flexion.

VI. Conclusion

In conclusion, we have presented the design of a multi-joint actuation platform for lower extremity soft ankle and hip exosuits designed to assist ankle plantar flexion and hip

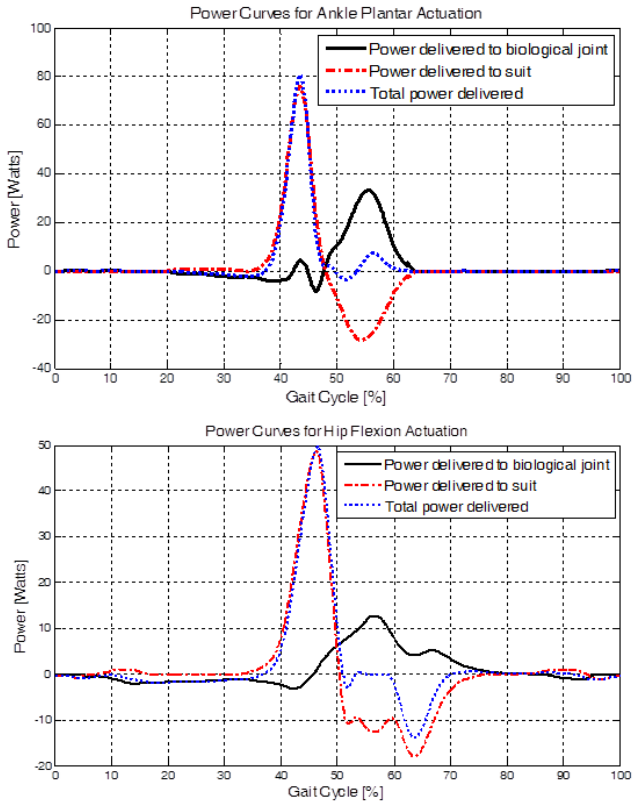

Figure 9 Average power delivered from the sytem, average power delivered to the suit and biological joints

flexion/extension during walking. With the modular, 6-DOF actuation platform, desired forces can be delivered to biological joints simultaneously through multiple Bowden cables. From the human walking experiments, it is demonstrated that desired force trajectory profiles, a percentage of Winter's biomechanics data [23], can be accurately followed with an admittance controller. The actuation platform includes integrated instrumentation on the robot and wearer side so that the power delivered to the suit and biological joints can be calculated. This enables us to compare the efficiency of different controllers directly.

Future work will focus on developing adaptive control strategies to optimize the force profile for each individual. Also, different control and assistive strategies for simultaneous multi-joint control of lower-limb exosuits will be tested to evaluate their effects on human biomechanics, metabolic cost and muscular activation. This will be performed with human subject studies measuring kinematics, kinetics and EMG.

VII. Acknowledgment

The authors would like to thank Robert Dyer, Arnar Larusson, and Ken Holt for their input during this project. The authors would also like to thank Copley Controls Corporation for providing Accelnet motor controllers.

References

[1] A. M. Dollar, and H. Herr, "Lower extremity exoskeletons and active orthoses: Challenges and state-of-the-art," *Robotics, IEEE Transactions on,* vol. 24, no. 1, pp. 144-158, 2008.

[2] A. B. Zoss, H. Kazerooni, and A. Chu, "Biomechanical design of the Berkeley lower extremity exoskeleton (BLEEX)," *Mechatronics, IEEE/ASME Transactions on,* vol. 11, no. 2, pp. 128-138, 2006.

[3] C. J. Walsh, K. Endo, and H. Herr, "A quasi-passive leg exoskeleton for load-carrying augmentation," *International Journal of Humanoid Robotics,* vol. 4, no. 03, pp. 487-506, 2007.

[4] J. E. Pratt, B. T. Krupp, C. J. Morse, and S. H. Collins, "The RoboKnee: an exoskeleton for enhancing strength and endurance during walking.", *Robotics and Automation, 2004. Proceedings. ICRA'04. 2004 IEEE International Conference on,* vol. 3, pp. 2430-2435. IEEE, 2004.

[5] H. Herr, "Journal of NeuroEngineering and Rehabilitation," *Journal of NeuroEngineering and Rehabilitation,* vol. 6, pp. 21, 2009.

[6] H. A. Quintero, R. J. Farris, C. Hartigan, I. Clesson, and M. Goldfarb, "A powered lower limb orthosis for providing legged mobility in paraplegic individuals," *Topics in spinal cord injury rehabilitation,* vol. 17, no. 1, pp. 25-33, 2011.

[7] G. S. Sawicki, and D. P. Ferris, "A pneumatically powered knee-ankle-foot orthosis (KAFO) with myoelectric activation and inhibition." *Journal of neuroengineering and rehabilitation* 6, no. 1 (2009): 23.

[8] W. van Dijk, H. van der Kooij, and E. Hekman, "A passive exoskeleton with artificial tendons: Design and experimental evaluation.", *Rehabilitation Robotics (ICORR), 2011 IEEE International Conference on*, pp. 1-6. IEEE, 2011.

[9] M. Goldfarb, and W. K. Durfee, "Design of a controlled-brake orthosis for FES-aided gait," *Rehabilitation Engineering, IEEE Transactions on,* vol. 4, no. 1, pp. 13-24, 1996.

[10] P. D. Neuhaus, J. H. Noorden, T. J. Craig, T. Torres, J. Kirschbaum, and J. E. Pratt, "Design and evaluation of mina: A robotic orthosis for paraplegics." *Rehabilitation Robotics (ICORR), 2011 IEEE International Conference on,* pp. 1-8. IEEE, 2011.

[11] S. K. Banala, S. K. Agrawal, and J. P. Scholz, "Active Leg Exoskeleton (ALEX) for gait rehabilitation of motor-impaired patients." *Rehabilitation Robotics, 2007. ICORR 2007. IEEE 10th International Conference on,* pp. 401-407. IEEE, 2007.

[12] S. K. Banala, S. H. Kim, S. K. Agrawal, and J. P. Scholz, "Robot assisted gait training with active leg exoskeleton (ALEX)," *Neural Systems and Rehabilitation Engineering, IEEE Transactions on,* vol. 17, no. 1, pp. 2-8, 2009.

[13] J. Hu, Y.-J. Lim, Y. Ding, D. Paluska, A. Solochek, D. Laffery, P. Bonato, and R. Marchessault, "An advanced rehabilitation robotic system for augmenting healthcare." *Engineering in Medicine and Biology Society, EMBC, 2011 Annual International Conference of the IEEE*, pp. 2073-2076. IEEE, 2011.

[14] H. Kawamoto, S. Lee, S. Kanbe, and Y. Sankai, "Power assist method for HAL-3 using EMG-based feedback controller." *Systems, Man and Cybernetics, 2003. IEEE International Conference on,* vol. 2, pp. 1648-1653. IEEE, 2003.

[15] A. Schiele, "Ergonomics of exoskeletons: Objective performance metrics." *EuroHaptics conference, 2009 and Symposium on Haptic Interfaces for Virtual Environment and Teleoperator Systems. World Haptics 2009. Third Joint,* pp. 103-108. IEEE, 2009.

[16] J. Cool, "Biomechanics of orthoses for the subluxed shoulder," *Prosthetics and Orthotics international,* vol. 13, no. 2, pp. 90-96, 1989.

[17] M. Wehner, B. Quinlivan, P. M. Aubin, E. Martinez-Villalpando, M. Baumann, L. Stirling, K. Holt, R. Wood, and C. Walsh, "A Lightweight Soft Exosuit for Gait Assistance," *Robotics and Automation (ICRA), 2013 IEEE International Conference on*, pp. 3347-3354, 2013.

[18] A. T. Asbeck, R. J. Dyer, A. F. Larusson, and C. J. Walsh, "Biologically-inspired Soft Exosuit," *Rehabilitation Robotics, 2013. ICORR 2013. IEEE 16th International Conference on*, Rehabilitation Robotics:[proceedings], vol. 2013, pp. 1-8. 2013.

[19] M. Wehner, Y.-L. Park, C. Walsh, R. Nagpal, R. J. Wood, T. Moore, and E. Goldfield, "Experimental characterization of components for active soft orthotics." *Biomedical Robotics and Biomechatronics (BioRob), 2012 4th IEEE RAS & EMBS International Conference on,* pp. 1586-1592. IEEE, 2012.

[20] G. S. Sawicki, and D. P. Ferris, "Mechanics and energetics of level walking with powered ankle exoskeletons," *Journal of Experimental Biology,* vol. 211, no. 9, pp. 1402-1413, 2008.

[21] G. S. Sawicki, and D. P. Ferris, "Powered ankle exoskeletons reveal the metabolic cost of plantar flexor mechanical work during walking with longer steps at constant step frequency," *Journal of Experimental Biology,* vol. 212, no. 1, pp. 21-31, 2009.

[22] M. Wehner, D. Rempel, and H. Kazerooni, "Lower Extremity Exoskeleton Reduces Back Forces in Lifting." *ASME*, 2009.

[23] D. A. Winter, Biomechanics and motor control of human gait: normal, elderly and pathological, 1991.

[24] G. A. Pratt, and M. M. Williamson, "Series elastic actuators." *Intelligent Robots and Systems 95.'Human Robot Interaction and Cooperative Robots', Proceedings. 1995 IEEE/RSJ International Conference on,* vol. 1, pp. 399-406. IEEE, 1995

[24] I. Galiana, F. L. Hammond, R. D. Howe, and M. B. Popovic. "Wearable soft robotic device for post-stroke shoulder rehabilitation: Identifying misalignments." *In Intelligent Robots and Systems (IROS), 2012 IEEE/RSJ International Conference on,* pp. 317-322. IEEE, 2012.

[25] A. Peer, "Design and Control of Admittance-Type Telemanipulation Systems." *VDI-Verlag,* 2008.